Chain Dimensions and Stiffness of Cellulosic and Amylosic Chains in an Ionic Liquid: Cellulose, Amylose, and an Amylose Carbamate in BmimCl

XinYue Jiang,[†] Shinichi Kitamura,[‡] Takahiro Sato,[†] and Ken Terao,[,†]*

[†]Department of Macromolecular Science, Graduate School of Science, Osaka University, 1-1 Machikaneyama-cho, Toyonaka, Osaka 560-0043, Japan.
[‡]Graduate School of Life and Environmental Sciences, Osaka Prefecture University, Gakuen-cho, Nakaku, Sakai, 599-8531, Japan.
* Corresponding Author. E-mail: kterao@chem.sci.osaka-u.ac.jp

ABSTRACT: Small-angle X-ray scattering measurements were made for cellulose, amylose, and amylose tris(ethylcarbamate) (ATEC) in an ionic liquid [1-butyl-3-methylimidazolium chloride (BmimCl)] at 25 °C to determine *z*-average mean-square radius of gyration $\langle S^2 \rangle_z$ and the particle scattering function $P(q)$. The obtained data were analyzed in terms of the wormlike chain model to estimate the Kuhn segment length λ^{-1} (the stiffness parameter, equivalent to twice of the persistence length) and the helix pitch (or helix rise) per residue h. The chain stiffness (λ^{-1}) was determined to be 7 ± 1 nm for cellulose, 3.5 ± 0.5 nm for amylose, and 7.5 ± 0.5 nm for ATEC. These values are almost the same or somewhat smaller than those of previously investigated systems, indicating these polymers have relatively high flexibility in the ionic liquid. It is reasonable to suppose that disruption of intramolecular hydrogen bonds of polysaccharide makes the main chain rather flexible in the ionic liquid.

Introduction

Since an ionic liquid, 1-butyl-3-methylimidazolium chloride (BmimCl), was found to dissolve cellulose,[1] it has been of great interest as the solvent of polysaccharides owing to the processibility of such materials. Ionic liquids are also suitable to investigate rheological properties or polymer dynamics of polysaccharides[2-7] because they have much higher viscosity and much lower volatility than common organic solvents. The chain conformation of polysaccharides in ionic liquids is prerequisite to discuss such dynamic properties from molecular point of view. Few examples are however reported to determine chain conformation of cellulose and amylose in some ionic liquids by light scattering[8-9] because test solutions for light scattering experiments have very high viscosity, low refractive index increment, and sometimes fluorescence from the solvent.

Such experimental difficulties can be removed in small-angle X-ray scattering (SAXS). Scattered X-ray intensities were found to be high enough in for dimensional analysis in our preliminary experiments. For the similar reason, polystyrene in some viscous solvents was investigated by small-angle neutron scattering.[10] We thus made solution SAXS measurements for cellulose, amylose, and amylose tris(ethylcarbamate) (ATEC) in BmimCl. Dissolution mechanisms of cellulose in this solvent have recently been investigated by molecular dynamics simulation.[11-13] The obtained particle scattering function data were analyzed in terms of the Kratky-Porod (KP) wormlike chain model[14] to determine the chain stiffness parameter λ^{-1} (the Kuhn segment length or twice of the persistence length).

The chain stiffness of cellulosic and amylosic chains in solution has been widely investigated in various solvents.[15-16] Cellulose is classified to as a semiflexible polymer of which λ^{-1} was thus determined in aqueous metal complexes,[17-20] in aqueous LiOH/urea,[21] in aqueous NaOH/urea,[22] in aqueous NaOH,[23] and in LiCl/amide solvents.[24-26] The λ^{-1} values vary from 8 to 50 nm depending on the solvent. Meanwhile, amylose behaves as a flexible polymer in various common organic solvents and aqueous solutions,[27-29] where λ^{-1} is 2 – 3 nm, (or 4 nm when analyzing the data in terms of the helical wormlike chain).[30] The exception is λ^{-1} = 18 nm in aqueous iron-sodium tartrate.[15, 18] Appreciable solvent dependent chain conformation was however found for amylose carbamate derivatives.[31-35] Those derivatives can form the intramolecular hydrogen bonding between carbamate groups on neighboring glucose units, depending on the solvent, which plays an important role in the chain stiffness. The chain stiffness parameters λ^{-1} obtained in this study for cellulose, amylose, and ATEC in BmimCl are compared with the literature results in different solvents, to argue the conformational nature of the polysaccharides in the ionic liquid.

Experimental Section

Samples and test solutions. *Cellulose*. Two cellulose samples, that is, Avicel PH-101 (Asahi Kasei) and 'Cellulose' (microcrystalline powder, Sigma) were used for this study without further purification and designated to be Cell38K and Cell37K, respectively. The weight-average molar mass M_w was estimated to be 3.8×10^4 g mol^{-1} and 3.7×10^4 g mol^{-1} for Cell38K and Cell37K, respectively, from the intrinsic viscosity $[\eta]$ in aqueous 6 wt % NaOH/4 wt % urea with the literature $[\eta] - M_w$ relationship.[22] The M_w value and the dispersity index $Đ$ defined as the ratio of M_w to the number average molar mass were also roughly estimated for Cell38K to be $M_w = 3.6 \times 10^4$ g mol^{-1} and $Đ = 1.6$ and for Cell37K to be $M_w = 4.2 \times 10^4$ g mol^{-1} and $Đ = 1.6$, from the M_w and $Đ$ of the corresponding phenylcarbamate derivative samples which were determined from the size-exclusion chromatography with light scattering and refractive index detectors (SEC-MALLS) in tetrahydrofuran (THF) with the refractive index increment being 0.170 cm^{3}g^{-1}.[36] The synthesis procedure of cellulose tris(phenylcarbamate) and SEC-MALLS measurements were substantially the same as those for cellulose tris(alkylcarbamate)s.[37] The slight difference in M_w may be occurred in the process of the purification of the phenylcarbamate derivative samples.

Amylose. Enzymatically synthesized two amylose samples[38] (ESA50K and ESA90K), which are the same as those recently used to synthesize amylose carbamate derivatives,[39] are chosen for this study. Their M_w values were estimated to be 5.0×10^4 g mol^{-1} and 9.3×10^4 g mol^{-1} for ESA50K and ESA90K, respectively, from $[\eta]$ in dimethylsulfoxide at 25 °C with the relationship between $[\eta]$ and M_w reported by Nakanishi et al.[27] The $Đ$ values are less than 1.2.[39]

Amylose tris(ethylcarbamate) (ATEC). Two previously investigated ATEC samples,[35] ATEC10K and ATEC150K were used for this study. Their $Đ$ values are less than 1.1.

Solvents and preparation of test solutions. BmimCl purchased from Wako was used as a solvent of which water content was 0.9 wt% referring to the company certificate. The solvent was dried in vacuum at 80 °C overnight. Thus, the actual water content may be smaller than the value according to the recent report for BmimCl with the similar purification (0.11 wt%).[40] It should be noted that this water content is still much lower than the value at which cellulose solution becomes turbid,[41] and furthermore the intrinsic viscosity of cellulose solution in a different ionic liquid including such a small amount of water was reported to be slightly larger than that in pure ionic liquid.[42] The resultant solvent was clear with no turbidity. Each sample which was dried in vacuum at room temperature for at least 12 hours was weighed with an electronic balance in a glass bottle and an appropriate amount of solvent was added. The resultant mixtures were stored

in a vacuum oven at 80-90 °C for 48 hours and then mixed with a magnetic stirrer bar for 24 hours at 60 °C to dissolve the sample. The obtained solutions were stored in a vacuum for 24 hours at 80 °C prior to the following SAXS measurements. As the preliminary solubility test for previously synthesized amylose and cellulose derivatives,[35-37, 39, 43-44] we found that amylose tris(phenylcarbamate), amylose 2-acetyl-3,6-bis(phenylcarbamate), and cellulose tris(ethylcarbamate) are soluble in BmimCl whereas cellulose tris(phenylcarbamate) is only soluble at 80 °C but the solution became turbid at room temperature. Furthermore, amylose tris(*n*-butylcarbamate), amylose tris(*n*-hexylcarbamate), and cellulose tris(*n*-butylcarbamate) are not soluble in BmimCl.

Small angle X-ray Scattering (SAXS) measurements. SAXS measurements were carried out for the above-mentioned solutions and the solvent at 25 °C at the BL40B2 beamline in SPring-8 (Hyogo, Japan). Although this temperature is lower than the melting temperature of BmimCl, due to supercooling, no aging effects were found in the measurement time scale in the range of temperature between −65 °C and 55 °C.[5] We note that the conformational change of cellulose should be still much quicker than the time scale even though the solvent viscosity is very high at the temperature, where it was reported to be 3.95 Pa s at 30 °C.[40] A Rigaku R-AXIS VII imaging plate was utilized to obtain two dimensional scattering intensity data. The wavelength, camera length, and accumulation time were chosen to be 0.10 nm, 4000 mm, and 300-600 s, respectively. Test solutions with several different polymer mass concentrations c ranging from 5×10^{-3} g cm^{-3} to 5×10^{-2} g cm^{-3} were measured for each polysaccharide sample in a quartz capillary cell with a diameter of 2 mmϕ. The lowest concentration for each sample was obviously lower than the overlap concentration c^* calculated from the resultant gyration radii while the highest concentration was somewhat lower or higher than c^* if we consider degradation of the cellulose sample as described in Results and Discussion. According to Kasabo et al.,[36] the Zimm plot for a cellulose derivative in an organic solvent has good linearity in the range of the concentration more than twice higher than c^*. It should be noted that solvent and test solutions are heated again to 80 °C to reduce the viscosity and relatively thick needles (1.2 mmϕ) were used to inject them into the capillary without air bubbles. Each measurement was started after it was stored for 5 − 20 min at room temperature (25 °C). Scattering profiles were not affected by this aging time difference. The circular average procedure was employed to obtain angular dependence of scattering intensity $I(q)$ which has been divided by the intensity of the direct beam at the lower end of the cell to correct both the incident light intensity and the transmittance, where q denotes the magnitude of the scattering vector. The same capillary was used to measure four solutions and the solvent to determine the excess scattering intensity $\Delta I(q)$ as the difference of $I(q)$ between each solution and the solvent. We note that the $I(q)$ data for solvent were substantially independent of q in the range of $q > 0.2$ nm^{-1} and slight higher $I(q)$ was observed in the lower q range. This is likely because of stray X-ray from the light source since similar behavior was also observed for tetrahydrofuran. The Berry square-root plot[45] was utilized to extrapolate the scattering intensity to infinite dilution to determine the z-average mean square radius of gyration $\langle S^2 \rangle_z$ and the particle scattering function $P(q)$.

Results and Discussion

Figure 1 illustrates the Berry plots of $[c/\Delta I(q)]^{1/2}$ vs q^2 for Cell38K and ESA50K in BmimCl both at 25 °C; note that substantially similar results were obtained if we choose the conventional Zimm plot to extrapolate $c/\Delta I(q)$ to zero concentration. Dashed lines in the figure indicate the

initial slope to determine $\langle S^2 \rangle_z$ and $P(q)$. The second virial coefficient A_2 was estimated from the slope of $[c/\Delta I(0)]^{1/2}$ (filled squares) using the M_w data mentioned in the former section with the same method reported in ref 46, in which the optical constant was estimated from $[c/\Delta I(0)]_{c=0}^{1/2}$ and the M_w value. The resultant $\langle S^2 \rangle_z$ and A_2 data are listed in Table 1 along with the M_w values. The latter values (A_2) are between 4×10^{-5} and 3.5×10^{-4} mol cm^{3}g^{-2}, indicating that the all polymer-solvent systems investigated in this study are good solvent systems. Actual values of M_w and A_2 for cellulose (and amylose) in BmimCl may be smaller and larger than these values, respectively, owing to the degradation during the dissolution process as we mention later.

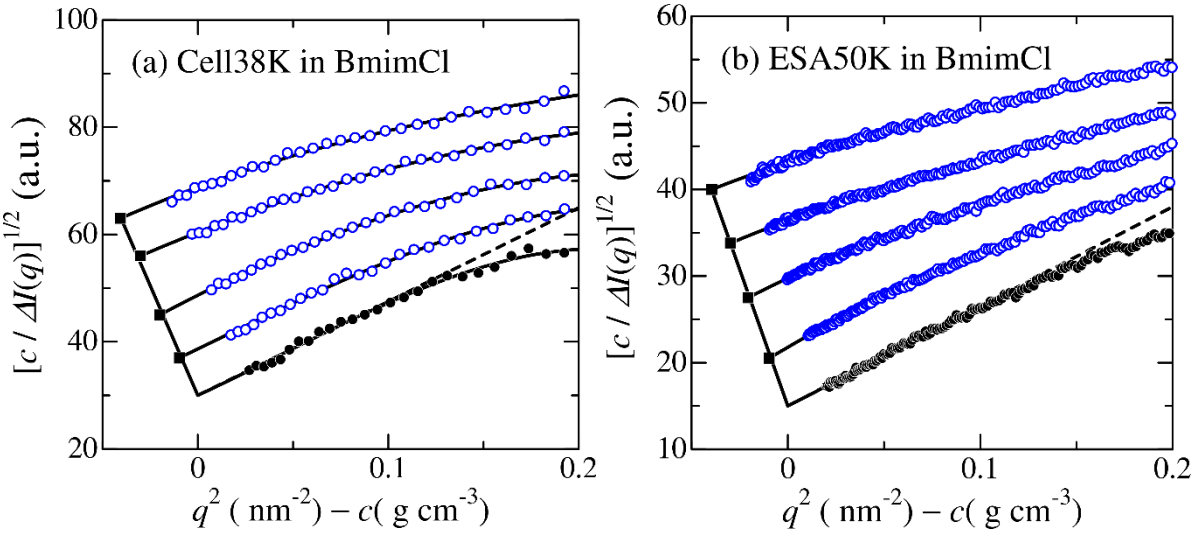

Figure 1. Square root Zimm plots (Berry plots) for Cell38K (a) and ESA50K (b) in BmimCl at 25 °C. Filled circles and squares, extrapolated values to $c = 0$ and $q^2 = 0$, respectively.

Table 1. Molecular Characteristics of Cellulose, Amylose, and ATEC samples in BmimCl at 25 ˚C

Samples	M_w (10^4 g mol^{-1})	$\langle S^2 \rangle_z^{1/2}$ (nm)	$\langle S^2 \rangle_{calc}^{1/2}$ (nm) [b]	A_2 (10^{-4} mol cm^3 g^{-2})
Cell37K	3.7	7.1	7.7 [c]	3.5 [d]
Cell38K	3.8	5.7	6.4 [c]	3.2 [d]
ESA50K	5.0	6.6	7.0	3.3 [d]
ESA90k	9.3	7.6	8.2	1.8 [d]
ATEC10K	1.02 [a]	2.7	2.1	1.5
ATEC150K	15.4 [a]	11.7	12.0	0.4

[a] ref 35. [b] Calculated by eq 2 with the parameters in Table 2. [c] z-average value with $Đ = 1.6$. [d] Assuming no degradation in the dissolution process.

The obtained $P(q)$ data are displayed in the form of the reduced Holtzer plot in Figure 2. The shape for almost all samples are typical for wormlike chains, namely, a flat plateau is found for

each sample in high q range with an appreciable peak at low q except for ATEC10K. The particle scattering function $P(q)$ for the touched-bead wormlike chain is expressed as[47-48]

$$P(q) = 9\left(\frac{2}{qd}\right)^6 \left(\sin\frac{qd}{2} - \frac{qd}{2}\cos\frac{qd}{2}\right)^2 P_0(q) \quad (1)$$

where $P_0(q)$ is the particle scattering function for the thin wormlike chain as follows.

$$P_0(q) = \frac{2}{L^2}\int_0^L (L-t)\, I\left(\lambda^{-1}q; \lambda t\right) dt \quad (2)$$

Here L, d, and $I(\lambda^{-1}q; \lambda t)$ are the contour length, the bead diameter, and the characteristic function of the KP chain which can be calculated by means of the approximate expression by Nakamura and Norisuye.[49-50] A curve fitting procedure was carried out for each sample to determine the three parameters, λ^{-1}, L, and d. Nicely fitted theoretical curves in Figure 2 indicate that the KP chain is a good model to explain the current $P(q)$ data. The three parameters summarized in Table 2 were unequivocally determined for almost all samples other than ATEC10K for which λ^{-1} was assigned the value obtained for the higher M_w sample, ATEC150K. Very small d values may be reasonable because this parameter reflects the electron density profiles of the chain cross section. Indeed, such small d was also found for other polymer-solvent systems[34, 37, 51] and it can be explained by some appropriate models such as the concentric double cylinder.[37, 52] We considered molar mass distribution for cellulose samples assuming log-normal distribution because their $Đ$ values (1.6) are somewhat larger than those for the other samples (1.1 – 1.2). The resultant theoretical values (red curves) slightly better fit the experimental data than the monodisperse case (blue curves).

Table 2. Wormlike Chain Parameters for Cellulose, Amylose, and ATEC samples in BmimCl at 25 ˚C.

sample	L (nm)	λ^{-1} (nm)	d (nm)
Cell37K	43 ± 3	7 ± 1 (9 ± 1)[b]	0
Cell38K	31 ± 2	7 ± 1 (9 ± 1)[b]	0
ESA50K	90 ± 15	3.5 ± 0.5	0
ESA90K	115 ± 15	3.7 ± 0.5	0
ATEC10K	9.0 ± 0.5	7.5 [a]	1.5 ± 0.1
ATEC150K	125 ± 10	7.5 ± 0.5	1.3 ± 0.1

[a] Assumed. [b] Parameter with $Đ$ = 1.

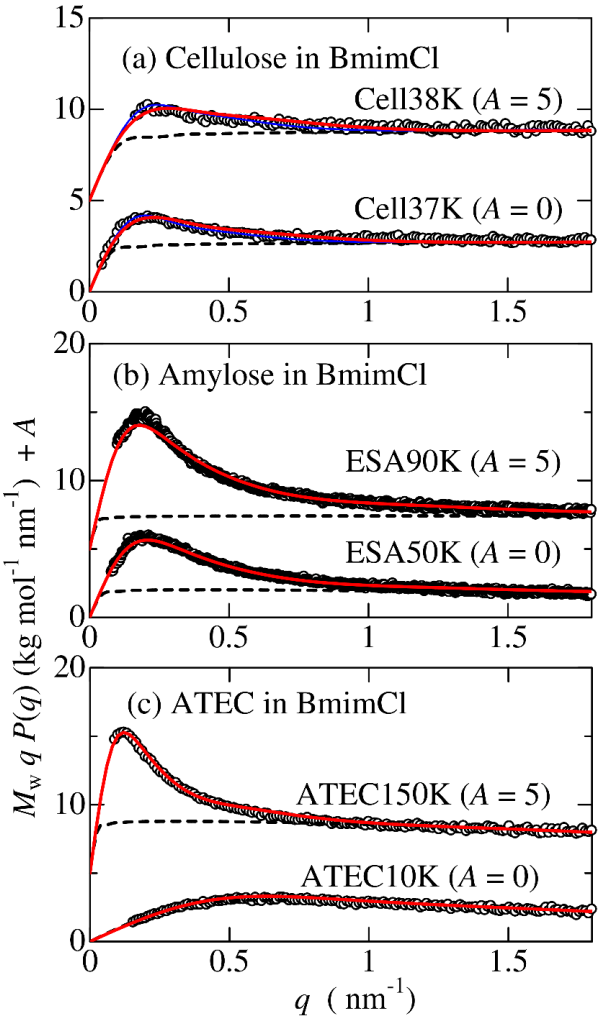

Figure 2. Reduced Holtzer plots for (a) cellulose in BmimCl, (b) amylose in BmimCl, and (c) ATEC in BmimCl at 25 °C. Solid and dashed curves indicate the theoretical values for the touched bead wormlike chain and the touched bead rigid rod, respectively. Red and blue curves in panel (a) correspond to $Đ = 1.6$ and $Đ = 1$, respectively.

The radius of gyration $\langle S^2 \rangle_{calc}$ for the KP wormlike chain is calculated from the following Benoit-Doty equation[53]

$$\left\langle S^2 \right\rangle = \frac{L}{6\lambda} - \frac{1}{4\lambda^2} + \frac{1}{4\lambda^3 L} - \frac{1}{8\lambda^4 L^2}\left[1 - \exp\left(-2\lambda L\right)\right] \tag{3}$$

for each sample with the parameters listed in Table 2. The resultant values are substantially close to that for the experimental values, indicating the obtained wormlike chain parameters consistently explain both $P(q)$ and $\langle S^2 \rangle_z$. Since the Kuhn segment number defined as λL for all samples are in the range from 1.2 to 31, the intramolecular excluded-volume effects may be negligible.[30, 54-55] Twice larger λ^{-1} value estimated for cellulose in 1-allyl-3-methylimidazolium chloride (AmimCl) in the previous report[8] is likely due to the excluded volume effect as well as the molar mass distribution. Indeed, the Kuhn segment number was roughly estimated for their sample to be 180

with λ^{-1} = 7 nm and the helix pitch per residue h = 0.515 nm. It is also noted that the local helical structure of amylose is rather unimportant for the current q range while it becomes more dominant for lower molar mass amylose at higher q range.[56] Thus, we do not show further analysis in terms of the helical wormlike chain model although this model is rather better to explain the viscosity behavior in dimethylsulfoxide.[27]

If we calculate h from L in Table 2 defined as $h = LM_0 / M_w$ with M_0 being molar mass per repeat unit, the h value is estimated as 0.19 and 0.13 nm for Cell37K and Cell38K, respectively. These are much smaller than those for cellulose in solution[17, 21-22] (0.45 – 0.51 nm), cellulose derivatives in solution[37] (0.40 – 0.51 nm), and cellulose molecules in crystal[57] (0.52 nm). This extremely small h values for cellulose in BmimCl suggest that degradation of cellulose molecules in the process of dissolution as depicted by some other researchers.[58-59] It is however noted that this degradation may not affect the determination of λ^{-1} unless $Đ$ does not change significantly. While ESA50K has relatively reasonable h value of 0.29 nm, which is close to that for amylose in solution 0.33 nm,[27] ESA90K has smaller h value of 0.20 nm. Degradation of amylose in the dissolution process is thus less likely than it is for cellulose. The main chain hydrolysis by solvent ionic liquid may become less prominent for polysaccharide derivatives. Indeed, the h value estimated for ATEC10K and ATEC150K to be 0.32 and 0.29 nm are not very different from those reported in other solvents, 0.35 – 0.38 nm.[35] The degradation of cellulose can also be proved from the data in Figure 1 with the doubly extrapolated method to $c = 0$ and $q^2 = 0$. If we assume ESA50K was not degraded in BmimCl and the contrast factor of cellulose is equivalent to amylose, the M_w values for ESA90K, Cell38K, and Cell37K may be estimated to be 6.2×10^4 g mol^{-1}, 1.3×10^4 g mol^{-1}, and 1.7×10^4 g mol^{-1}, respectively. Reasonable h values are calculated from the M_w values both for amylose (0.30 nm) and cellulose (0.40 nm). Concentration range for the SAXS measurements was therefore estimated to be $0.3\ c^* < c < 2.0\ c^*$ for cellulose, $0.14\ c^* < c < 0.7\ c^*$ for amylose, and $0.05\ c^* < c < 1.0\ c^*$ for ATEC if we calculated c^* by $c^* = 3M_w/4\pi N_A\langle S^2\rangle_z^{3/2}$ with N_A being the Avogadro number. The obtained chain stiffness parameters for the three polymers in BmimCl are summarized in Table 3 with the literature values in various solvents. The following is the discussion for each system.

Cellulose in BmimCl. Although cellulose is not soluble in common organic and inorganic solvents owing to the intramolecular hydrogen bonding, several kinds of aqueous alkaline solutions containing metal complexes were developed. Representative Kuhn segment lengths reported in last two decades are listed in Table 3.[9, 17-18, 20-22, 25] The currently obtained λ^{-1} value in BmimCl is the smallest of the solvent systems. Conformational energy calculations[60-62] demonstrated that the cellulosic chain takes an extended conformation with λ^{-1} as large as 60 nm, but if the bond angle of the glucosidic bridge slightly increases from that in the crystalline state, a new energetically stable rotational state appears which acts as a kink and remarkably reduces λ^{-1}.[62] The experimental values of λ^{-1} in Table 3 are much smaller than 60 nm, which may be explained by the quasi-stable (kink) conformation as well as the underestimated torsion angle fluctuation. According to the modern molecular dynamics for an oligo cellulose, intramolecular hydrogen bonds of cellulose disrupted in BmimCl.[11, 13] Similar reduction of intramolecular hydrogen bonds was also reported in other ionic liquids.[63] Smaller λ^{-1} for cellulose in BmimCl than in aqueous 6 wt % NaOH/4 wt % urea is most likely due to the decrease of intramolecular hydrogen bonds since such hydrogen bonds may remain in the latter solvent.[64]

Amylose in BmimCl. Native amylose extracted from starch has some branching structure.[65-66] We thus compared λ^{-1} data for enzymatically synthesized amylose (ESA) in dimethylsulfoxide (DMSO) and a metal complex. Conformational energy calculations for amylose[56, 67-70] give us a

single broad minimum in the conformational energy map, which provides 0.8 – 4 nm for λ^{-1} of which the value depends on the force field.[56] The estimated λ^{-1} range from the simulation includes the experimental results in BmimCl, as well as common organic solvents and aqueous solutions reported. The λ^{-1} value in FeTNa is much larger than these values. This is likely because carboxy groups of tartrate may form hydrogen bonds with hydroxy groups of amylose, which may severely restrict the fluctuation of the internal rotation about the glucosidic linkage.

ATEC in BmimCl. The fraction of the intramolecular hydrogen bonding C=O and N-H groups determines the chain stiffness of amylose alkylcarbamate derivatives, so that λ^{-1} depends significantly on the hydrogen-bonding ability of the solvent.[32, 35, 44] Methanol is an intramolecular hydrogen-bonding breaking solvent for the amylose derivatives, and infrared (IR) absorption demonstrated almost no intramolecular hydrogen bonds of ATEC in methanol.[35] The chain stiffness in BmimCl is close or slightly smaller than that in methanol. It is thus concluded that the flexibility of the ATEC chain in BmimCl comes from the breakage of the intramolecular hydrogen bonds of ATEC although IR absorption by BmimCl makes difficult to check the fraction of the intramolecular hydrogen bonding.

Table 3. Kuhn Segment Length λ^{-1} for Cellulose, Amylose, and ATEC in Various Solvents

polymer	solvent	λ^{-1} (nm)	Reference
cellulose	1-butyl-3-methylimidazolium chloride (BmimCl)	7 ± 1	this work
	aqueous $Cd(en)_3(OH)_2$ (cadoxen)	8	9, 71
	0.5 M aqueous $Cu(en)_3(OH)_2$ (en = ethylenediamine) (Cuen)	9	20
	aqueous $Ni(tren)(OH)_2$ [tren = tris(2-aminoethyl)amine]	10	17
	4.6 wt % LiOH/15 wt % urea in water	12	21
	6 wt % NaOH/4 wt % urea in water	12	22
	aqueous $Cu(NH_3)_4(OH)_2$ (cuoxam)	13	17
	aqueous $Cd(tren)(OH)_2$	16	17
	DMAc with 0.5% LiCl	16	20
	1,3-dimethyl-2-imidazolidinone (DMI) with 1% LiCl	18	25
	dimethylacetoamide (DMAc) with 8% LiCl	18	25
	aqueous iron-sodiumtartrate (FeTNa)	21	18
amylose (ESA)	BmimCl	3.5 ± 0.5	this work
	dimethylsulfoxide (DMSO)	2.4 (4)[a]	27
	DMSO with 43.5 vol % acetone	2.4 (4)[a]	28-29
	formamide	2.4 (4)[a]	28-29
	0.5 M aqueous NaOH	2.4 (4)[a]	28-29
	water	2.4 (4)[a]	28-29
	aqueous FeTNa	18	18

ATEC	BmimCl	7.5 ± 0.5	this work
	methanol	9	35
	2-methoxyethanol	14	35
	L-ethyl lactate	15	35
	D-ethyl lactate	27	35
	tetrahydrofuran (THF)	33	35

[a] For the helical wormlike chain.

Conclusion

The chain stiffness parameter λ^{-1} was successfully determined for cellulose, enzymatically synthesized amylose (ESA), and amylose tris(ethylcarbamate) (ATEC) in an ionic liquid (BmimCl). While some chain degradation was observed especially for cellulose, clear scattering data were obtained for all systems. Analyses in terms of the wormlike chain shows that all the three polymers have rather flexible main chain in BmimCl while cellulose and ATEC behave as semiflexible or stiff chains in other solvents. This is most likely due to the reduction of the intramolecular hydrogen bonds and the resultant increase of the conformational fluctuation.

Acknowledgment

The authors thank Dr. Noboru Ohta (SPring-8) and Dr. Rintaro Takahashi (Kitakyushu Univ.) for SAXS measurements. The synchrotron radiation experiments were performed at the BL40B2 in SPring-8 with the approval of the Japan Synchrotron Radiation Research Institute (JASRI) (Proposal Nos. 2014B1087, 2015A1179, 2015B1100, 2015B1674, and 2016A1053). This work was partially supported by JSPS KAKENHI Grant No. 25410130.

References

1. Swatloski, R. P.; Spear, S. K.; Holbrey, J. D.; Rogers, R. D. Dissolution of cellulose with ionic liquids. *J. Am. Chem. Soc.* **2002,** *124*, 4974-5.
2. Kuang, Q. L.; Zhao, J. C.; Niu, Y. H.; Zhang, J.; Wang, Z. G. Celluloses in an ionic liquid: the rheological properties of the solutions spanning the dilute and semidilute regimes. *J Phys Chem B* **2008,** *112*, 10234-40.
3. Horinaka, J.; Yasuda, R.; Takigawa, T. Entanglement Properties of Cellulose and Amylose in an Ionic Liquid. *J. Polym. Sci., Part. B: Polym. Phys.* **2011,** *49*, 961-965.
4. Chen, X.; Zhang, Y. M.; Wang, H. P.; Wang, S. W.; Liang, S. W.; Colby, R. H. Solution rheology of cellulose in 1-butyl-3-methyl imidazolium chloride. *J. Rheol.* **2011,** *55*, 485-494.
5. Maeda, A.; Inoue, T.; Sato, T. Dynamic Segment Size of the Cellulose Chain in an Ionic Liquid. *Macromolecules* **2013,** *46*, 7118-7124.
6. Ahn, Y.; Kwak, S. Y.; Song, Y.; Kim, H. Physical state of cellulose in BmimCl: dependence of molar mass on viscoelasticity and sol-gel transition. *Physical chemistry chemical physics : PCCP* **2016,** *18*, 1460-9.
7. Sescousse, R.; Le, K. A.; Ries, M. E.; Budtova, T. Viscosity of cellulose-imidazolium-based ionic liquid solutions. *J Phys Chem B* **2010,** *114*, 7222-8.
8. Chen, Y.; Zhang, Y. M.; Ke, F. Y.; Zhou, J. H.; Wang, H. P.; Liang, D. H. Solubility of neutral and charged polymers in ionic liquids studied by laser light scattering. *Polymer* **2011,** *52*, 481-488.

9. Maeda, A. Conformation and Dynamics of the Cellulose Chain in Ionic Liquids. Ph.D. Thesis, Osaka University, 2014.
10. Lodge, T. P.; Hermann, K. C.; Landry, M. R. Coil Dimensions of Polystyrenes in Isorefractive Viscous Solvents by Small-Angle Neutron-Scattering. *Macromolecules* **1986,** *19*, 1996-2002.
11. Xu, H.; Pan, W.; Wang, R.; Zhang, D.; Liu, C. Understanding the mechanism of cellulose dissolution in 1-butyl-3-methylimidazolium chloride ionic liquid via quantum chemistry calculations and molecular dynamics simulations. *J. Comput. Aided Mol. Des.* **2012,** *26*, 329-37.
12. Gross, A. S.; Bell, A. T.; Chu, J. W. Entropy of cellulose dissolution in water and in the ionic liquid 1-butyl-3-methylimidazolim chloride. *Physical chemistry chemical physics : PCCP* **2012,** *14*, 8425-30.
13. Mostofian, B.; Cheng, X.; Smith, J. C. Replica-exchange molecular dynamics simulations of cellulose solvated in water and in the ionic liquid 1-butyl-3-methylimidazolium chloride. *J Phys Chem B* **2014,** *118*, 11037-49.
14. Kratky, O.; Porod, G. Rontgenuntersuchung Geloster Fadenmolekule. *Recl. Trav. Chim. Pays-Bas* **1949,** *68*, 1106-1122.
15. Burchard, W. Light Scattering from Polysaccharides as Soft Materials. In *Soft Matter Characterization*, Borsali, R.; Pecora, R., Eds. Springer Netherlands: 2008; pp 463-603.
16. Kamide, K. *Cellulose and cellulose derivatives*. Elsevier: 2005.
17. Saalwachter, K.; Burchard, W.; Klufers, P.; Kettenbach, G.; Mayer, P.; Klemm, D.; Dugarmaa, S. Cellulose solutions in water containing metal complexes. *Macromolecules* **2000,** *33*, 4094-4107.
18. Seger, B.; Aberle, T.; Burchard, W. Solution behaviour of cellulose and amylose in iron-sodiumtartrate (FeTNa). *Carbohydr. Polym.* **1996,** *31*, 105-112.
19. Burchard, W.; Habermann, N.; Klüfers, P.; Seger, B.; Wilhelm, U. Cellulose in Schweizer's Reagent: A Stable, Polymeric Metal Complex with High Chain Stiffness. *Angewandte Chemie International Edition in English* **1994,** *33*, 884-887.
20. Kes, M.; Christensen, B. E. A re-investigation of the Mark-Houwink-Sakurada parameters for cellulose in Cuen: a study based on size-exclusion chromatography combined with multi-angle light scattering and viscometry. *J. Chromatogr. A* **2013,** *1281*, 32-7.
21. Cai, J.; Liu, Y. T.; Zhang, L. N. Dilute solution properties of cellulose in LiOH/urea aqueous system. *J. Polym. Sci., Part. B: Polym. Phys.* **2006,** *44*, 3093-3101.
22. Zhou, J. P.; Zhang, L. N.; Cai, J. Behavior of cellulose in NaOH/urea aqueous solution characterized by light scattering and viscometry. *J. Polym. Sci., Part. B: Polym. Phys.* **2004,** *42*, 347-353.
23. Kamide, K.; Saito, M.; Kowsaka, K. Temperature-Dependence of Limiting Viscosity Number and Radius of Gyration for Cellulose Dissolved in Aqueous 8-Percent Sodium-Hydroxide Solution. *Polym. J.* **1987,** *19*, 1173-1181.
24. McCormick, C. L.; Callais, P. A.; Hutchinson, B. H. Solution studies of cellulose in lithium chloride and N,N-dimethylacetamide. *Macromolecules* **1985,** *18*, 2394-2401.
25. Yanagisawa, M.; Isogai, A. SEC-MALS-QELS study on the molecular conformation of cellulose in LiCl/amide solutions. *Biomacromolecules* **2005,** *6*, 1258-65.
26. Bianchi, E.; Ciferri, A.; Conio, G.; Cosani, A.; Terbojevich, M. Mesophase formation and chain rigidity in cellulose and derivatives. 4. Cellulose in N,N-dimethylacetamide-lithium chloride. *Macromolecules* **1985,** *18*, 646-650.

27. Nakanishi, Y.; Norisuye, T.; Teramoto, A.; Kitamura, S. Conformation of Amylose in Dimethyl-Sulfoxide. *Macromolecules* **1993,** *26*, 4220-4225.
28. Norisuye, T. Viscosity Behavior and Conformation of Amylose in Various Solvents. *Polym. J.* **1994,** *26*, 1303-1307.
29. Burchard, W. Das Viskositatsverhalten Von Amylose in Verschiedenen Losungsmitteln .24. *Makromol. Chem.* **1963,** *64*, 110-125.
30. Yamakawa, H.; Yoshizaki, T. *Helical Wormlike Chains in Polymer Solutions, 2nd ed.* Springer: Berlin, Germany, 2016.
31. Fujii, T.; Terao, K.; Tsuda, M.; Kitamura, S.; Norisuye, T. Solvent-Dependent Conformation of Amylose Tris(phenylcarbamate) as Deduced from Scattering and Viscosity Data. *Biopolymers* **2009,** *91*, 729-736.
32. Sano, Y.; Terao, K.; Arakawa, S.; Ohtoh, M.; Kitamura, S.; Norisuye, T. Solution properties of amylose tris(n-butylcarbamate). Helical and global conformation in alcohols. *Polymer* **2010,** *51*, 4243-4248.
33. Tsuda, M.; Terao, K.; Nakamura, Y.; Kita, Y.; Kitamura, S.; Sato, T. Solution Properties of Amylose Tris(3,5-dimethylphenylcarbamate) and Amylose Tris(phenylcarbamate): Side Group and Solvent Dependent Chain Stiffness in Methyl Acetate, 2-Butanone, and 4-Methyl-2-pentanone. *Macromolecules* **2010,** *43*, 5779-5784.
34. Arakawa, S.; Terao, K.; Kitamura, S.; Sato, T. Conformational change of an amylose derivative in chiral solvents: amylose tris(n-butylcarbamate) in ethyl lactates. *Polym. Chem.* **2012,** *3*, 472-478.
35. Terao, K.; Maeda, F.; Oyamada, K.; Ochiai, T.; Kitamura, S.; Sato, T. Side-Chain-Dependent Helical Conformation of Amylose Alkylcarbamates: Amylose Tris(ethylcarbamate) and Amylose Tris(n-hexylcarbamate). *J. Phys. Chem. B* **2012,** *116*, 12714-12720.
36. Kasabo, F.; Kanematsu, T.; Nakagawa, T.; Sato, T.; Teramoto, A. Solution properties of cellulose tris(phenyl carbamate). 1. Characterization of the conformation and intermolecular interaction. *Macromolecules* **2000,** *33*, 2748-2756.
37. Jiang, X. Y.; Ryoki, A.; Terao, K. Dimensional and hydrodynamic properties of cellulose tris (alkylcarbamate)s in solution: Side chain dependent conformation in tetrahydrofuran. *Polymer* **2017,** *112*, 152-158.
38. Kitamura, S.; Yunokawa, H.; Mitsuie, S.; Kuge, T. Study on Polysaccharide by the Fluorescence Method .2. Micro-Brownian Motion and Conformational Change of Amylose in Aqueous-Solution. *Polym. J.* **1982,** *14*, 93-99.
39. Terao, K.; Fujii, T.; Tsuda, M.; Kitamura, S.; Norisuye, T. Solution Properties of Amylose Tris(phenylcarbamate): Local Conformation and Chain Stiffness in 1,4-Dioxane and 2-Ethoxyethanol. *Polym. J.* **2009,** *41*, 201-207.
40. Kuang, Q.; Zhang, J.; Wang, Z. Revealing long-range density fluctuations in dialkylimidazolium chloride ionic liquids by dynamic light scattering. *J Phys Chem B* **2007,** *111*, 9858-63.
41. Mazza, M.; Catana, D. A.; Vaca-Garcia, C.; Cecutti, C. Influence of water on the dissolution of cellulose in selected ionic liquids. *Cellulose* **2009,** *16*, 207-215.
42. Le, K. A.; Sescousse, R.; Budtova, T. Influence of water on cellulose-EMIMAc solution properties: a viscometric study. *Cellulose* **2012,** *19*, 45-54.
43. Tsuda, M.; Terao, K.; Kitamura, S.; Sato, T. Solvent-dependent conformation of a regioselective amylose carbamate: Amylose-2-acetyl-3,6-bis(phenylcarbamate). *Biopolymers* **2012,** *97*, 1010-1017.

44. Terao, K.; Murashima, M.; Sano, Y.; Arakawa, S.; Kitamura, S.; Norisuye, T. Conformational, Dimensional, and Hydrodynamic Properties of Amylose Tris(*n*-butylcarbamate) in Tetrahydrofuran, Methanol, and Their Mixtures. *Macromolecules* **2010,** *43*, 1061-1068.
45. Berry, G. C. Thermodynamic and Conformational Properties of Polystyrene .I. Light-Scattering Studies on Dilute Solutions of Linear Polystyrenes. *J. Chem. Phys.* **1966,** *44*, 4550-4564.
46. Jiang, Y.; Zhang, X.; Miao, B.; Yan, D. The study of the structure factor of a wormlike chain in an orientational external field. *J. Chem. Phys.* **2015,** *142*, 154901.
47. Nagasaka, K.; Yoshizaki, T.; Shimada, J.; Yamakawa, H. More on the Scattering Function of Helical Wormlike Chains. *Macromolecules* **1991,** *24*, 924-931.
48. Burchard, W.; Kajiwara, K. The Statistics of Stiff Chain Molecules. I. The Particle Scattering Factor. *Proc. R. Soc. London, Ser. A* **1970,** *316*, 185-199.
49. Nakamura, Y.; Norisuye, T. Scattering Function for Wormlike Chains with Finite Thickness. *J. Polym. Sci., Part. B: Polym. Phys.* **2004,** *42*, 1398-1407.
50. Nakamura, Y.; Norisuye, T. Brush-Like Polymers. In *Soft Matter Characterization*, Borsali, R.; Pecora, R., Eds. Springer Netherlands: 2008; pp 235-286.
51. Nagata, Y.; Hasegawa, H.; Terao, K.; Suginome, M. Main-Chain Stiffness and Helical Conformation of a Poly(quinoxaline-2,3-diyl) in Solution. *Macromolecules* **2015,** *48*, 7983-7989.
52. Livsey, I. Neutron-Scattering from Concentric Cylinders - Intraparticle Interference Function and Radius of Gyration. *Journal of the Chemical Society-Faraday Transactions Ii* **1987,** *83*, 1445-1452.
53. Benoit, H.; Doty, P. Light Scattering from Non-Gaussian Chains. *J. Phys. Chem.* **1953,** *57*, 958-963.
54. Norisuye, T.; Fujita, H. Excluded-Volume Effects in Dilute Polymer Solutions. XIII. Effects of Chain Stiffness. *Polym. J.* **1982,** *14*, 143-147.
55. Norisuye, T.; Tsuboi, A.; Teramoto, A. Remarks on Excluded-Volume Effects in Semiflexible Polymer Solutions. *Polym. J.* **1996,** *28*, 357-361.
56. Shimada, J.; Kaneko, H.; Takada, T.; Kitamura, S.; Kajiwara, K. Conformation of Amylose in Aqueous Solution: Small-Angle X-ray Scattering Measurements and Simulations. *J. Phys. Chem. B* **2000,** *104*, 2136-2147.
57. Nishiyama, Y.; Langan, P.; Chanzy, H. Crystal Structure and Hydrogen-Bonding System in Cellulose Iβ from Synchrotron X-ray and Neutron Fiber Diffraction. *J. Am. Chem. Soc.* **2002,** *124*, 9074-9082.
58. Gazit, O. M.; Katz, A. Dialkylimidazolium ionic liquids hydrolyze cellulose under mild conditions. *ChemSusChem* **2012,** *5*, 1542-8.
59. Zhang, H.; Wu, J.; Zhang, J.; He, J. S. 1-Allyl-3-methylimidazolium chloride room temperature ionic liquid: A new and powerful nonderivatizing solvent for cellulose. *Macromolecules* **2005,** *38*, 8272-8277.
60. Yathindra, N.; Rao, V. S. R. Configurational statistics of polysaccharide chains. Part II. Cellulose. *Biopolymers* **1970,** *9*, 783-790.
61. Goebel, K. D.; Harvie, C. E.; Brant, D. A. The Configurational Statistics of Cellulosic Chains. *Appl. Polym. Symp.* **1976,** *28*, 671-691.
62. Yanai, H.; Sato, T. Local Conformation of the Cellulosic Chain in Solution. *Polym. J.* **2006,** *38*, 226-233.

63. Payal, R. S.; Balasubramanian, S. Dissolution of cellulose in ionic liquids: an ab initio molecular dynamics simulation study. *Physical chemistry chemical physics : PCCP* **2014,** *16*, 17458-65.
64. Jiang, Z.; Fang, Y.; Xiang, J.; Ma, Y.; Lu, A.; Kang, H.; Huang, Y.; Guo, H.; Liu, R.; Zhang, L. Intermolecular interactions and 3D structure in cellulose-NaOH-urea aqueous system. *J. Phys. Chem. B* **2014,** *118*, 10250-7.
65. Takeda, Y.; Maruta, N.; Hizukuri, S. Examination of the Structure of Amylose by Tritium Labeling of the Reducing Terminal. *Carbohydr. Res.* **1992,** *227*, 113-120.
66. Takeda, Y.; Tomooka, S.; Hizukuri, S. Structures of Branched and Linear-Molecules of Rice Amylose. *Carbohydr. Res.* **1993,** *246*, 267-272.
67. Goebel, C. V.; Brant, D.; Dimpfl, W. The Conformational Energy of Maltose and Amylose. *Macromolecules* **1970,** *3*, 644-654.
68. Brant, D.; Dimpfl, W. A Theoretical Interpretation of the Aqueous Solution Properities of Amylose and Its Derivatives. *Macromolecules* **1970,** *3*, 655-664.
69. Jordan, R. C.; Brant, D. A.; Cesàro, A. A Monte Carlo study of the amylosic chain conformation. *Biopolymers* **1978,** *17*, 2617-2632.
70. Nakata, Y.; Kitamura, S.; Takeo, K.; Norisuye, T. Conformation of Amylose and Excluded-Volume Effects on Its Chain Dimensions. *Polym. J.* **1994,** *26*, 1085-1089.
71. Henley, D. A Macromolecular Study of Cellulose in Solvent Cadoxen. *Arkiv for Kemi* **1961,** *18*, 327-392.

For Table of Contents Use Only

Chain Dimensions and Stiffness of Cellulosic and Amylosic Chains in an Ionic Liquid: Cellulose, Amylose, and an Amylose Carbamate in BmimCl

XinYue Jiang, Shinichi Kitamura, Takahiro Sato, and Ken Terao